

Mid-infrared intersublevel absorption of vertically electronically coupled InAs quantum dots

C. Kammerer, S. Sauvage,^{a)} G. Fishman, and P. Boucaud

Institut d'Électronique Fondamentale, UMR CNRS 8622, Bâtiment 220, Université Paris-Sud, 91405 Orsay, France

G. Patriarche and A. Lemaître

Laboratoire de Photonique et Nanostructures UPR 20, CNRS, Route de Nozay, F-91460 Marcoussis, France

(Received 23 December 2004; accepted 16 September 2005; published online 20 October 2005)

We have studied mid-infrared intersublevel absorption of samples containing two layers of vertically self-aligned, self-assembled InAs quantum dots separated by a thin GaAs barrier. Samples with coupled quantum dots exhibiting different average size between the two layers are investigated. The electronically coupled quantum dot absorption is compared with the absorption of a reference sample containing uncoupled quantum dots. Electronically coupled quantum dots present a spectrally narrow absorption line (~ 20 meV full width at half maximum) mainly polarized along the growth axis in the range 110–150 meV. This absorption is attributed to the bound-to-bound transition between bonding (symmetric-like) and antibonding (antisymmetric-like) s state combinations of the double quantum dot structure. This assignment is supported by the electronic structure of the coupled quantum dots as calculated by the three-dimensional resolution of the Schrödinger equation written in the 8-band $\mathbf{k}\cdot\mathbf{p}$ envelope function formalism. © 2005 American Institute of Physics. [DOI: 10.1063/1.2117621]

Semiconductor quantum dots (QDs), such as self-assembled InAs islands inserted into a GaAs matrix, are three-dimensionally confined nanostructures which exhibit quantized electronic levels with an ultra-sharp density of states. Isolated QDs have attracted a lot of interest in the last years because they could be used for devices such as lasers¹ and photodetectors.² QDs have also been considered as possible candidates for the implementation of solid-state quantum bits and the realization of entangled states and quantum gates involving two-qubit operations, in particular in QD molecules, i.e., pairs of electronically coupled QDs.^{3–5} A way to realize coupled QDs is to use the strain coupling between two closely spaced QD layers. The growth conditions needed to obtain such QD pairs are now well known.^{6,7} There have been a lot of work in the past years devoted to the demonstration of the electronic coupling in such a pair of QDs, particularly illustrating that coupling QDs represents a mean of tailoring the electronic structure.^{8–12} The splitting of the excitonic ground state into two optically active transitions (the separation energy of which increases with decreasing the barrier thickness between the two QDs) has been demonstrated mainly through photoluminescence spectroscopy but this splitting is small and for the ground state, it is difficult to extract it from the inhomogeneous broadening. Furthermore, the electronic coupling between two QDs in a pair depends on their relative level energies and, for instance, it is still technologically challenging to tune precisely two QD ground state energy levels.¹³

In this work we study the mid-infrared absorption of two vertically stacked QD ensembles. We compare the absorption of coupled QD layers (sample A) with uncoupled QD layers (sample B). We show that coupled quantum dots present an additional narrow absorption line mainly polarized along the

growth axis ($E\parallel z$), which is attributed to a transition between the bonding and antibonding s level combinations of the double QD structure. This result differs from a recent experimental work where an in-plane polarized absorption was observed instead for coupled QDs in the same energy range.⁸ We perform three-dimensional calculations of the double QD electronic structure using 8 band $\mathbf{k}\cdot\mathbf{p}$ theory that supports the assignment of this mainly z -polarized absorption. These results show that the observation of a relatively spectrally narrow and strong absorption mainly polarized along the growth axis is a signature of a tunnel coupling existing between stacked QDs.

The investigated samples A and B are grown by molecular beam epitaxy on a (001) oriented GaAs substrate. Sample A consists of 15 double InAs QD layer periods separated by 50 nm thick GaAs barriers. The period is constituted by two QD layers separated by a nominal 3 nm thick deposited GaAs barrier. The first QD layer corresponds to the deposition of 2.2 InAs monolayers (ML) and the second QD layer to 1.1 InAs ML. The wafer was not rotated during the second QD layer growth in order to get a thickness gradient of the deposited InAs along an arbitrarily chosen wafer axis. The size mismatch between the QDs from the two layers is then varying along this axis. Sample B is grown in the same conditions as the first QD layer of sample A in order to get similar QDs in the two samples for the first layer. It consists of 30 QD layers separated by 50 nm thick GaAs barriers. The dot density in these samples, as estimated from separate atomic force microscope measurements, is around 2×10^{10} cm⁻². A doping of the QDs was provided by a delta-planar modulation doping 2 nm below the QD layers resulting in a nominal doping of two carriers per double QD for sample A and two carriers per dot for sample B.

In the following, we will show results obtained on two different points from wafer A referenced to as *BigSmall* point and *BigBig* point (named after the relative QD sizes in the

^{a)}Electronic mail: sebastien.sauvage@ief.u-psud.fr

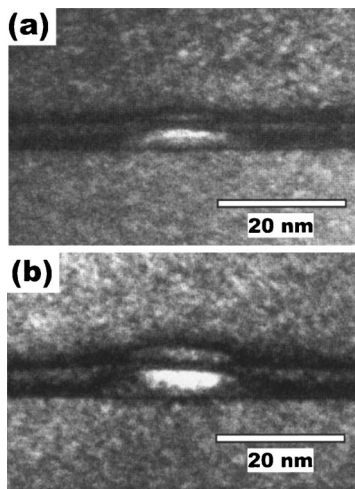


FIG. 1. Cross-sectional (002) dark-field TEM images of sample A showing the coupled QDs from the two different points (a) *BigSmall* and (b) *BigBig*.

stacked QD pair). Cross-sectional transmission electron microscopy (TEM) (002) dark field images from these two points are shown in Fig. 1. From these images, composition of indium can be directly determined from the study of contrast between InGaAs and GaAs regions according to a parabolic law.¹⁵ 9% in-plane shape anisotropy is observed in a reference single QD plane sample. The nominal thickness of deposited GaAs between the two QD layers is 3 nm and results in a 0.7 nm observed vertical separation between the two QDs.

The intersublevel absorption of samples A and B was measured with a Fourier-transform infrared spectrometer. The backside and the end facets of the samples were polished to give a 45° wave guide providing 12 passes through the dot layers for sample A and 10 passes for sample B. A scheme of the waveguide geometry can be seen on the upper part of Fig. 2.

Figure 2 depicts the transmission spectra at 130 K for the two different *BigSmall* and *BigBig* points of sample A and for one point of sample B. The straight line is obtained for a *p*-polarized light (70% polarized along the growth axis and 30% polarized in the layer plane), and the dashed line for in-plane polarized light (*s* polarization). Each transmission spectrum is normalized by the transmission spectrum at 300 K recorded on the same point of the same sample. The transmission spectrum at 300 K is used as a reference background because the thermal depopulation of the dots at room temperature leads to the strong quenching of the QD related spectral features observed at low temperature.¹⁶

For a polarization along the growth axis, a weak and broad absorption can be observed above 160 meV for sample B (uncoupled QDs). From the amplitude of the absorption and assuming a total transfer of electron from the doping layers to QDs, the absorption cross section σ for one QD layer is estimated to be about $3 \times 10^{-15} \text{ cm}^2$. For sample A (coupled QDs), a narrow absorption resonance is instead observed at 144 meV for *BigSmall* point and at 109 meV for *BigBig* point with a full width at half maximum broadening of only ~ 20 meV. This resonance is mainly polarized along the growth axis. From the amplitude of the absorption peak, the absorption cross section for two coupled layers is estimated to be about $2 \times 10^{-14} \text{ cm}^2$ which corresponds to a large dipole moment of $d_z \sim 2 \text{ e.nm}$.

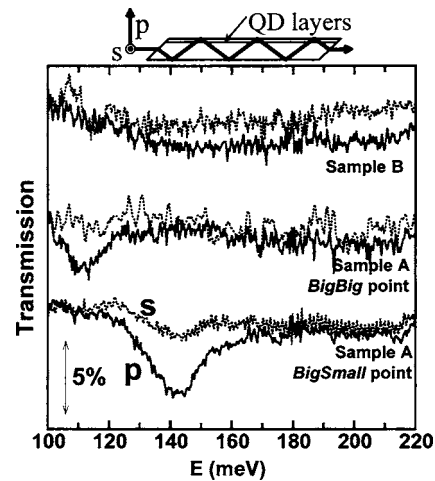


FIG. 2. Upper part: Scheme of the waveguide geometry used for infrared measurements. Lower part: Transmission spectra at 130 K normalized by transmission spectra at 300 K from two different points of sample A and from one point of sample B. Straight line: For *p* polarization and dashed line for *s* polarization.

For a polarization in the layer plane, a strong absorption could also be measured in sample B in the range 40–50 meV (not shown). This absorption is detected for one light pass through the sample in a normal incidence configuration. It consists of two cross-polarized components centered at 46 meV and 49.5 for a radiation polarized along the $[\bar{1}10]$ and $[110]$ direction. Their energy separation is about 4 meV and their full width at half maximum (FWHM) 6 meV. The magnitude of the absorption is $\sim 9\%$ which corresponds to an absorption cross section $\sigma \sim 7 \times 10^{-14} \text{ cm}^2$. In the same way for sample A, *BigBig* point, two absorption lines could be observed: One centered at 47.5 meV (with FWHM 5 meV and $\sim 4\%$ absorption amplitude) which corresponds to a dipole moment of 3.5 e.nm, and another one at lower energy which is not fully resolved because of the 43 meV cut-off energy of the spectrometer. Finally for sample A, *BigSmall* point, an absorption line centered around 45 meV is observed and not fully resolved for the same reason.

All these results show that absorption resonances polarized in the layer plane are observed both for uncoupled and coupled quantum dots in the same 40–50 meV energy range. On the contrary, for polarization along the growth axis, a spectrally narrow absorption resonance could only be measured for coupled quantum dots, both in the case of coupled dots with very different and similar size and composition. We attribute this difference to a signature of the electronic coupling.

In uncoupled QDs the in-plane polarized absorption corresponds to a bound to bound absorption between the *s-p* levels of the QDs.^{16,17} The splitting of the *s-p* absorption line is attributed to a combination of the elongated geometry of the dots and the piezoelectric field originating from the dot pyramidal shape and alloy disorder.¹⁸ The absorption along the growth axis is attributed to a bound-to-continuum transition between the *s* level and the wetting layer states.

When two QDs are electronically coupled, in particular by decreasing the vertical separation d between the two dots, the electronic levels localized in each dot start to hybridize with the levels of the other dot (in a molecular-like description) and start to give rise to bonding and antibonding levels with increasingly large energy separation and oscillator

strength when d decreases.^{14,19} Here the term bonding and antibonding refer to the relative sign (or phase) of the wave function in the two dots: same sign for bonding (symmetric-like), opposite sign for antibonding (antisymmetric-like).

The assignment of this resonance to a specific intersublevel transition is based on the calculation of the electronic structure of the coupled QD system given by the three-dimensional resolution of the envelope function Schrödinger equation written within the 8-band $\mathbf{k}\cdot\mathbf{p}$ formalism.² For these calculations, the realistic size, shape and composition parameters of the QDs are given by the TEM images. The strong electron-phonon coupling, giving rise to the formation of polarons, is not considered here.¹⁷ A scheme of the calculated energy levels is shown on Fig. 3 for the two QDs corresponding to *BigSmall* point taken separately and for the same coupled QDs with a barrier separation thickness of 0.7 nm. The s levels from the two QDs taken separately have very different energies (the energy separation is 125 meV). With a GaAs separation thickness of 0.7 nm, the QDs are electronically coupled, the s level energy from the first QD is lowered and it is increased for the second QD (the energy changes for these levels are 8 and 10 meV, respectively). The calculated electronic envelope wave functions for these two states are shown in Fig. 3. A careful analysis of the wave functions indicates that, depending on the sizes and composition, the mixing also involves contribution from other states than s states, those states in the lower dot which are in energy resonance with the s state of upper dot.

The only possible intersublevel transitions with a non-negligible dipole length (i.e., greater than 0.5 nm) are calculated at 42 and 49 meV with a polarization in the layer plane (3.7 and 3.4 nm dipole length) and at 143 meV with polarization along the growth axis between the two bonding and antibonding states with a 1.6 nm dipole length. These calculations confirm that the narrow absorption line detected for sample A for polarization along the growth axis is characteristic of the electronic coupling of the QDs.

The energy separation between these bonding and antibonding states depends on the tunnel coupling strength between the two QDs but also on the compositions and sizes of the two QDs, which determine the relative position of the s levels from the QDs taken separately. The calculations show that the contribution of the electronic coupling on the bonding-antibonding transition energy is of the order of 20 meV for the *BigSmall* point, i.e., much smaller than that energy. The observed infrared resonance energies therefore mainly originate from the composition and size of the coupled quantum dots. One notes that, should the quantum dots be much more separated, the dipole length of the bonding-to-antibonding transition would be very small because of the vanishingly small overlapping of the envelope wave functions. Though the transition energy is not mainly driven by the electronic coupling, but rather simply by the composition and sizes of the quantum dots, the observation of a strong oscillator strength is, however, as demonstrated by the calculation, a direct consequence of this electronic coupling. At last, the energy separation between the s levels of the two separate QDs is smaller for *BigBig* point than for *BigSmall* point, with a calculated energy of 87 meV, therefore, leading to an observed (109 meV) and calculated

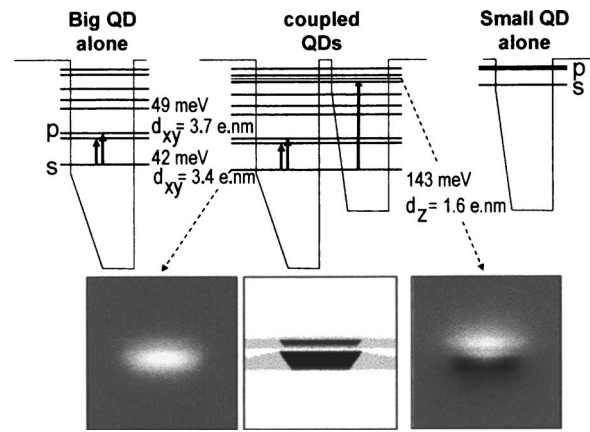


FIG. 3. Upper part: calculated energy levels for isolated QDs and coupled QDs of sample A, *BigSmall* point. The arrows show the allowed intersublevel transitions with a dipole moment greater than 0.5 e.nm. Lower part: Scheme of the QD pair shape used in the calculations and conduction band projection of the envelope wave functions for two levels of the coupled QD system in a plane containing the growth axis. The electronic envelope wave function is negative in the black region, positive in the white region and vanishing in the grey region.

(108 meV) smaller energy separation between the bonding and antibonding states. The in-plane polarized component of the *BigSmall* 144 meV absorption line is attributed to the 20% light depolarization occurring through the propagation in the wave guide, as measured and confirmed using crossed polarizers at the front and back of the waveguide.

¹M. Grundmann, *Nano-Optoelectronics* (Springer, New York, 2002).

²P. Boucaud and S. Sauvage, *C. R. Phys.* **4**, 1133 (2003).

³E. Biolat, R. C. Iotti, P. Zanardi, and F. Rossi, *Phys. Rev. Lett.* **85**, 5647 (2000).

⁴M. Bayer, P. Hawrylak, K. Hinzer, S. Fafard, M. Korkusinski, Z. R. Wasilewski, O. Stern, and A. Forchel, *Science* **291**, 451 (2001).

⁵P. Borri, W. Langbein, U. Woggon, M. Schwab, M. Bayer, S. Fafard, Z. Wasilewski, and P. Hawrylak, *Phys. Rev. Lett.* **91**, 267401 (2003).

⁶Q. Xie, A. Madhukar, P. Chen, and N. P. Kobayashi, *Phys. Rev. Lett.* **75**, 2542 (1995).

⁷G. S. Solomon, J. A. Trezza, A. F. Marshall, and J. S. Harris, Jr., *Phys. Rev. Lett.* **76**, 952 (1996).

⁸A. M. Adawi, E. A. Zibik, L. R. Wilson, A. Lemaître, J. W. Cockburn, M. S. Skolnick, M. Hopkinson, G. Hill, S. L. Liew, and A. G. Cullis, *Appl. Phys. Lett.* **82**, 3415 (2003).

⁹I. Shtrichman, C. Metzner, B. D. Gerardot, W. V. Schoenfeld, and P. M. Petroff, *Phys. Rev. B* **65**, 081303(R) (2002).

¹⁰G. Ortner, M. Bayer, A. Larionov, V. B. Timofeev, A. Forchel, Y. B. Lyanda-Geller, T. L. Reinecke, P. Hawrylak, S. Fafard, and Z. Wasilewski, *Phys. Rev. Lett.* **90**, 086404 (2003).

¹¹P. Boucaud, J. B. Williams, K. S. Gill, M. S. Sherwin, W. V. Schoenfeld, and P. M. Petroff, *Appl. Phys. Lett.* **77**, 4356 (2000).

¹²S. Fafard, M. Spanner, J. P. McCaffrey, and Z. R. Wasilewski, *Appl. Phys. Lett.* **76**, 2268 (2000).

¹³B. D. Gerardot, I. Shtrichman, D. Hebert, and P. M. Petroff, *J. Cryst. Growth* **252**, 44 (2003).

¹⁴A. Vasanelli, M. De Giorgi, R. Ferreira, R. Cingolani, and G. Bastard, *Physica E (Amsterdam)* **11**, 41 (2001).

¹⁵A. Lemaître, G. Patriarche, and F. Glas, *Appl. Phys. Lett.* **85**, 3717 (2004).

¹⁶F. Bras, P. Boucaud, S. Sauvage, G. Fishman, and J. M. Gérard, *Appl. Phys. Lett.* **80**, 4620 (2002).

¹⁷S. Hameau, J. N. Isaia, Y. Guldner, O. Verzellen, R. Ferreira, G. Bastard, J. Zeman, and J. M. Gérard, *Phys. Rev. B* **65**, 085316 (2002).

¹⁸M. A. Migliorato, D. Powell, S. L. Liew, A. G. Cullis, P. Navaretti, M. J. Steer, M. Hopkinson, M. Fearn, and J. H. Jefferson, *J. Appl. Phys.* **96**, 5169 (2004).

¹⁹M. Korkusinski and P. Hawrylak, *Phys. Rev. B* **63**, 195311 (2001).